

Detection and Segmentation of Breast Cancer Using Auto Encoder Deep Neural Networks

Aqeel Ali Abed¹, Mehran Emadi²

1- Department of Computer Engineering, Isfahan (Khorasgan) Branch, Islamic Azad University, Isfahan, Iran.
Email: aqeel2hlal@gmail.com

2- Department of Electrical Engineering, Mobarakeh Branch, Islamic Azad University, Mobarakeh, Iran.
Email: emadi.mehran49@gmail.com (Corresponding author)

Received: 27 July 2023

Revised: 23 August 2023

Accepted: 25 September 2023

ABSTRACT:

Breast cancer is the most common type of cancer among women worldwide. If diagnosed by a doctor in the early stages, it can save the patient's life. Ultrasound imaging is one of the most widely used diagnostic tools for diagnosing and classifying breast abnormalities. However, accurate segmentation of the ultrasound image is a challenging problem due to the artifacts created on the ultrasound image. Although deep learning-based methods have been able to overcome some of these challenges, the accuracy of tumor region detection in this image is still low. In this paper, we have proposed approaches for breast ultrasound image segmentation based on auto-encoder deep neural network. The proposed method has two parts. The classification section to determine the image with cancerous tissue and the tumor segmentation section to segment the desired area. which will be shown in the network output of the encoder itself. The proposed method has been evaluated qualitatively and quantitatively. The superiority of the proposed method with accuracy and dice criteria is 89 and 90 percent, respectively which shows the effectiveness of this method in diagnosis.

KEYWORDS: Segmentation, Breast Masses, Ultrasound Images, Automatic Encoder Neural Networks.

1. INTRODUCTION

Breast cancer (BrC) is the second leading cause of cancer-related deaths among women worldwide. As stated by the World Health Organization (WHO), by 2020 BrC was diagnosed in 2.3 million women and 685,000 deaths were recorded worldwide [1]. In addition, WHO predicts that the number of new patients will grow by seventy percent (70%) in the next twenty years. BrC is the fifth leading cause of death among all types of cancer, including colorectal, liver, lung, and stomach cancers [2]. Due to lack of awareness in South Asian countries, BrC is considered a growing epidemic. Most of the time, this disease remains hidden, and most patients are detected in the advanced and acute stages of the disease, and the survival rate in these stages reaches 30%. Therefore, it is very vital and necessary to use a cost-effective and automatic health service method that can diagnose the disease accurately and early [1-4]. Accurate and early diagnosis of this disease will increase prognosis and increase the survival rate by 50%. The use of medical imaging to effectively diagnose BrC is more common than other methods. Histopathology (Hp) images, breast X-ray

images (mammography), sonogram (ultrasound imaging) and magnetic resonance imaging (MRI) are widely used to diagnose BrC [5]. Ultrasound imaging system involves exposing body parts to high-frequency sound waves to create images of the internal structure of the human body. An ultrasound scan does not use ionizing radiation like a mammogram, making it a safer alternative [5]. Ultrasound scanning also produces relatively high resolution images [6]. The correct diagnosis of cancerous tumors requires correct identification of breast tissue changes in each stage of the disease, as well as identification of their type in ultrasound images [7]. Doctors and pathologists play an important role in the reliable diagnosis of cancerous tumors in these images [7]. Unfortunately, in most cases, due to human errors, negligence or distance from specialist doctors, especially in remote areas, BrC is not diagnosed correctly in the early stages, but it is very important to diagnose it in the early stages [8-11]. In the meantime, researchers have been able to help doctors by using Computer aided diagnosis (CAD) systems for early detection of breast tumors in

ultrasound images [18-26]. These systems are readily available, fast, reliable and cost-effective in the early detection of BrC. About a decade has passed since the development of CAD systems in increasing the accuracy of BrC detection and its usage rate has increased to more than 20% [19]. This system helps physicians and radiologists to detect, categorize and isolate abnormalities using different imaging methods and reduce the mortality rate from 30% to 70% [20]. In recent decades, these systems have been exploited with more complex and newer approaches such as artificial intelligence techniques for cancer diagnosis. Deep learning (DL) is widely recognized as one of these approaches and its efficiency has been shown in cancer prediction as well as in prognosis [21]. DL has a high diagnostic accuracy for breast cancer detection in mammography and ultrasound breast cancer imaging [22]. Currently, the clinical treatment of BrC relies on DL for higher accuracy. In recent years, many studies have used deep learning to detect BrC from various medical images [23-25]. In 2017, Cruz-Roa, Angel et al presented a classification approach to detect the presence and extent of breast cancer on digital whole-slide histopathology images using the ConvNet classifier [26]. In 2016, Zhang et al presented a research in which they used deep learning (DL) architecture for classification and shear-wave elastography (SWE) to automatically extract learned image features from data to distinguish between benign and malignant breast tumors [27]. In 2018, Liu et al. have described a new solution to improve the classification performance for each dataset based on Convolutional Neural Networks (CNN) [28]. In 2018, Xiao et al. demonstrated a novel scheme that integrates a deep learning-based unsupervised feature extraction algorithm, stack autoencoders, with a stacked autoencoders, with a support vector machine (SAE-SVM), for breast cancer detection [29]. In 2019, Zhou et al. used Convolutional Neural Networks (CNN) to segment breast ultrasound images into four main tissues: skin, fibroglandular tissue, mass, and fat tissue, on three-dimensional breast ultrasound images [30]. In 2021, Eco-Minaro et al. have used the CNN-based auto-encoder method to minimize the false information in the feature extraction process and improve the performance result [31]. In 2022, Hesa Nasser et al. presented a new breast cancer classification approach based on fully convolutional networks (FCN) and beta wavelet autoencoder (BWAE) [32]. Ragab et al. in a study in 2022 developed a clinical decision support system based on deep learning for the diagnosis and classification of breast cancer Ensemble Deep-Learning-Enabled Clinical Decision Support System for Breast Cancer Diagnosis and (EDLCDS-BCDC) using ultrasound images [33]. Jabeen et al. in 2022 for

classification BrC uses deep learning and merges the best selected features in ultrasound images [34]. In 2022, Khan et al. proposed a MultiNet framework based on the concept of transfer learning to classify different types of breast cancer [35]. Since the neural network's receptive field is fixed, it cannot use global and local information simultaneously during the training process, so multi-scale images are used as input images. In this way, the model can simultaneously learn macro- and micro-scale features and achieve better classification ability. In this research, an AE + SoftMax model structure is proposed, where AE extracts the effective input features by copying the input to the output through learning. As a result, effective feature extraction can be done and feature selection mentality can be avoided. In addition, the model training time and memory consumption are much less than CNN. In the following, this article is segmented as follows. In the second part, autoencoder neural networks will be introduced. In the third part, the proposed method is presented. Finally, in the fourth part, the evaluation of the proposed method will be done. In the fifth part, the conclusion of the article will be stated.

2. DEEP LEARNING ARCHITECTURES BASED ON AUTOMATIC ENCODER

An autoencoder neural network is an unsupervised learning algorithm that compresses the input into a hidden space representation by applying a backpropagation algorithm with target values similar to the inputs. It consists of two parts:

- i. The network encoder section that condenses the input into a hidden space representation expressed by the [mathematical processing error] function.
- ii. A network decoder part that reconstructs the input from the hidden space representation.

Compression is achieved by constraining the hidden layer to have dimensions less than the input layer. Such a network is known as incomplete. A lower dimension of the hidden layer results in the network learning the most salient features in the training data. Alternatively, a scattering constraint can also be applied to achieve similar results by keeping neurons in the hidden layer inactive most of the time. In autoencoder-based deep learning approaches, the input consists of an image that is sampled to obtain a lower-dimensional hidden representation, enabling the autoencoder to be trained and learn on the compressed form of the images. The architecture of the autoencoder is shown in Figure 1.

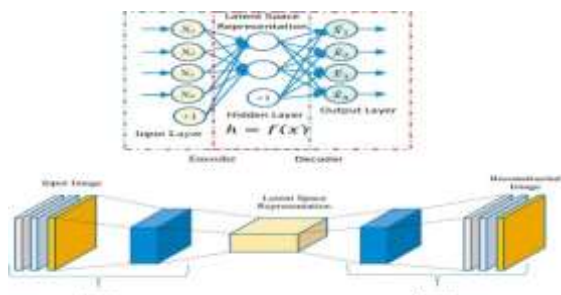


Fig. 1. Autoencoder architecture with vector and image inputs.

One of the challenges in automatic encoders is that there are more nodes in the hidden layer than the number of input values. This is the risk of learning the null network or identity function where the output is equal to the input. To solve this problem, automatic denoising encoders are used, where the data is deliberately distorted by randomly assigning about 30-50% of the input values as zeros. The actual values reduced to zero depend on the size of the data and the number of nodes in the network. When determining the loss function, the output is compared to the original input, thus eliminating the risk of learning a null function. The applications of autoencoders are relatively limited due to the discontinuity in the hidden space representations, which does not allow its use as a generative model. To solve this problem, variable autoencoders were introduced. In variable autoencoder, the encoder output is not a single encoded vector, but two encoded vectors. One is the mean vector and the other is the standard deviation vector. These vectors act as parameters of a random variable from which the output coded vector is sampled. This allows the decoder to correctly decode encoded values, even in the presence of small variations of the same input during training. The stochastic nature of the autoencoder ensures that the representation of the hidden space is continuous with the design, thus allowing random interpolation and sampling.

3. BLOCK DIAGRAM OF THE PROPOSED METHOD

The main goal of this research is segmentation of ultrasound images with the help of a deep neural network of self-encrypting convolutional neural networks. In this regard, the quality of the image should be improved with the help of pre-processing methods. Then the proposed deep structure is defined in segmentation. The general block diagram of the proposed method is shown in Figure 2.

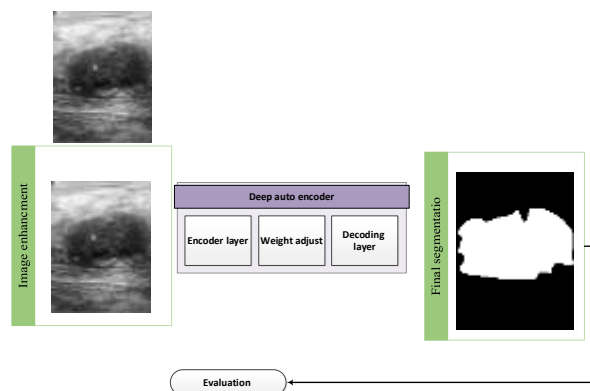


Fig. 2. Block diagram of the proposed segmentation method.

Ultrasound images often contain a large amount of speckle noise and artifacts, resulting in relatively low contrast and signal-to-noise ratio (SNR). Therefore, a preprocessing method is required to reduce the speckle in advance to improve the subsequent segmentation performance. Several filtering approaches have been proposed in the literature to reduce speckle in BUS images while preserving edge detail. Among these methods, the most successful are those based on anisotropic diffusion and bilateral filtering [17]. Bidirectional filter is usually used to improve image quality. By using a range kernel combined with a spatial kernel, the filter is able to smooth images without excessive edge blurring. It is shown that by adapting the width of the range kernel at each pixel, the gain capacity of the filter can be increased. In this paper, a fast algorithm for grayscale images is proposed for this so-called adaptive two-way filter, which is otherwise computationally expensive and computationally complex. This can be extended to color filtering using channelwise processing. Figure 3 shows an example of the image.

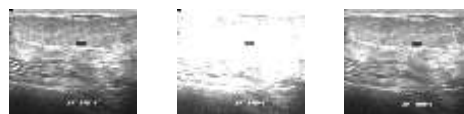


Fig. 3. An example of the improved image in the filtering method

4. PROPOSED DEEP NEURAL NETWORK

The network consists of two branches, a classification branch and a segmentation branch, as shown in Figure 4. These two branches are common in encoder layers. The segmentation part of the network is based on the structure of U-Net29 with DenseNet30 as the backbone. The network is U-shaped, which mainly consists of an encoder, a decoder, and jumpers. The encoder reduces the spatial dimension (feature scale) with maximum integration and extracts the context features. The decoder recovers the up-sampling spatial

dimension and propagates the background information to higher resolution layers. The skip connection transfers the features in the encoder directly to the decoder of the same scale to recover possible information loss. The hop connection and upsampling features are connected together in the decoder and propagated to the next layer. Specifically, the encoder consists of four dense blocks and three integration layers, and the decoder consists of three dense blocks and three upsampling layers. Dense blocks consist of several dense transform blocks, which include two batch normalization layers and two convolution layers with kernel sizes of 1 and 3, respectively. Four dense blocks in the encoder consist of 3, 4, 8 and 12 transform blocks, respectively. Three dense blocks in the decoder consist of 8, 4 and 3 conversion blocks, respectively.

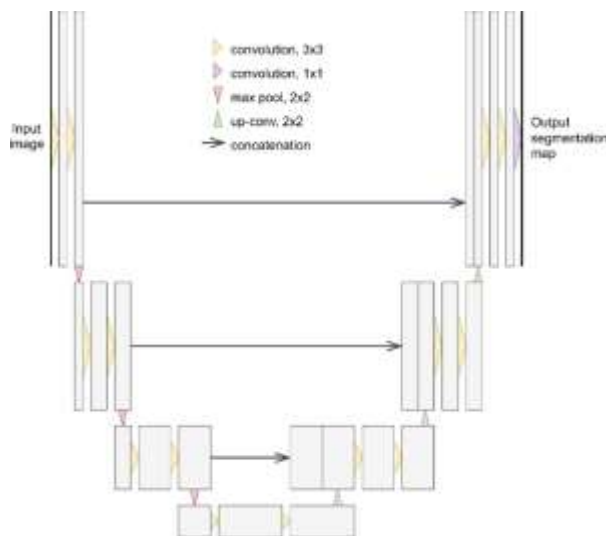


Fig. 4. Block diagram of the proposed autoencoder structure.

Data sets used for model training were combined to increase the generalization ability of the model. All images, both normal and abnormal, were fed to the network to optimize the parameters. Before feeding to the grid, the images were resized to 256x256 and the pixel values were normalized to [1, -1]. Images were also subjected to random horizontal rotation to enhance the data. Multi-task loss including classification loss and segmentation loss were used to optimize our model. The classification loss was the binary cross-entropy loss function, and the segmentation loss was a combination of the pixel binary cross-entropy loss function and the dice loss function. And the background in terms of segmentation and makes the education process more stable. The segmentation loss function in a single image is defined as:

$$L_{BCE}(y, t) = - \sum_{ij} (t \log(y) + (1 - t) \log(1 - y)) \quad (1)$$

$$L_{Dice}(y, t) = 1 - \frac{2 * \sum_{ij} yt + 1}{\sum_{ij} y + \sum_{ij} yt + 1}$$

$$L_{seg} = L_{BCE} + L_{Dice}$$

Here t is the ground truth and y is the predicted outcome. i and j represent a pixel on the image.

During training, 10x validation was used:

- i. The images in the training dataset were randomly divided into tenfold.
- ii. Nine were used for training and one was left for validation.
- iii. The model with the highest similarity coefficient of the validation dice was selected as the final model.
- iv. Statistics of average results and standard deviation were calculated in ten experiments.

An adaptive estimation of moment (ADAM) optimizer with an initial learning rate of 0.001 was used to train the model. In order to train the neural network with 15 convolution layers, 12 layers of this convolution network have 3 x 3 filters and also three dense layers with 256, 128 and 2 weights. There are also two Softmax since there is an invariant feature in the transfer in pool layers, pool layers are used in this research. Because the method [14] has been used to adjust the weights in the desired network. Which has a batch size of 128 and cross entropy function. The Rectifier Linear Unit(ReLU) activity function is used to initialize the weights, which have a Gaussian distribution with zero mean. The training rate is also selected with an initial value of 0.0001. In order to avoid over fitting training, this description has been increased to 0.3. The number of epochs is considered to be 1000 at most. The rule with the least error will be considered as the source model. This network will be trained with patch model. Also, for the final segmentation, the density layers have been changed to their convolution equivalent, i.e. FCN. Fully connected Network (FCN) networks account for redundant and redundant computations in neighboring parts. Figure 6-3 shows the proposed final structure for segmentation.

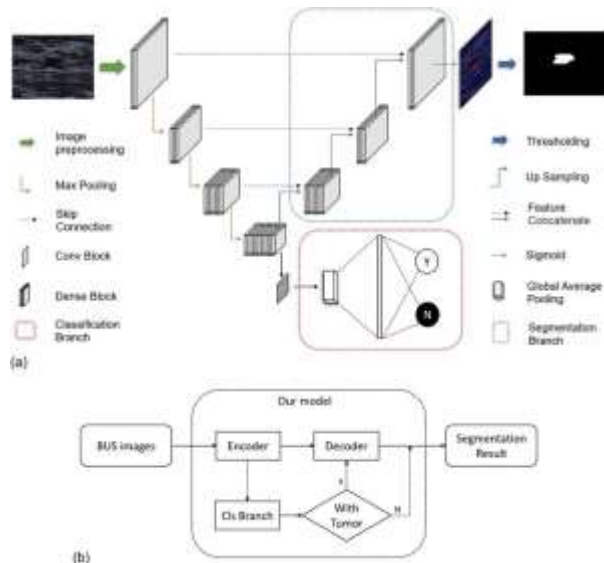


Fig. 5. The final structure for segmentation.

5. RESULTS

Identifying and diagnosing the type of tumor in breast ultrasound images can reduce human error and high diagnosis costs. Also, to minimize physical damage due to pathology in the chest. In this research, an efficient method for detecting the type of tumor has been presented, in which tumor is zoned in the breast image for various reasons, including the partial volume effect, the similarity of the brightness of some areas of the tumor with the mammary glands and variation in shape, and random position. Challenging. However, in this research, segmentation has been done using autoencoder neural networks. In order to evaluate the proposed method, the database has been used. Some examples of data are shown in Figure 6. Also, the specifications of the database are shown in Table 1.

Table 1. Characteristics of the research database.

Case	Number of images
Benign	487
Malignant	210
Normal	133
Total	780

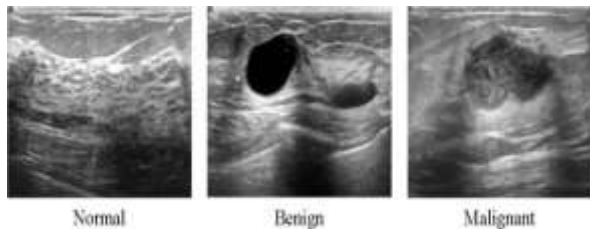


Fig. 6. Examples of ultrasound image data in the database.

In order to evaluate the proposed method, DICE criteria, Jaccard similarity index (JSI) and accuracy (ACC) are used, because DICE not only evaluates the number of correctly labeled pixels, but also the accuracy of the segmentation boundaries. The following relationship represents the DICE criterion.

$$Dice = \frac{2 * (TP)}{2 * (TP) + FN + FP} * 100 \tag{Y}$$

Jaccard similarity index (JSI) is also known as intersection-over-unity (IoU) and is calculated as the following relationship.

$$J(A, B) = \frac{|A \cap B|}{|A \cup B|} \tag{Y}$$

In the above relation, A is the segmented image and B is the real wallpaper. Accuracy is the ratio of the total number of correctly classified pixels (the sum of TP positive and TN false positive) to the total number of image pixels.

$$ACC = \frac{TP + TN}{TP + TN + FP + FN} \tag{Y}$$

5.2. EVALUATION OF THE PROPOSED METHOD

The performance of the proposed approach was compared with several state-of-the-art segmentation models including [34]U-Net, UNet++, [35]CE-Net, [36]CPFNet, [37]and FPNN. The role of the classification branch of the basic model is a U-Net with DenseNet as the basis of all methods, which is similar to the model proposed in this research, but the classification branch is removed. The basic model is called model-2. All these models were trained on the aforementioned datasets in the same way as our model. For further experiments, Model-2 was trained with only positive images (with tumor) in the dataset and the resulting model was named as Model-2-pos. It is worth noting that this particular method of Model-2-pos training is commonly used in tumor segmentation studies. Table 2 and 3 shows the segmentation results of eight different models. It can be seen that the first six models, including U-Net, UNet++, CE-Net, CPFNet, FPNN, and Model-2, show similar metrics, while our model significantly outperforms these six models in all metrics. For example, the DSCs of the first six models range from 0.743 to 0.826, while that of the proposed method is 0.898.

Table 2. Comparison of segmentation results in the SY test data set (mean ± standard deviation).

Model	DSC	JSI	ACC
U-Net ²⁹	0.746 ± 0.015	0.644 ± 0.012	0.789 ± 0.020
UNet++ ³⁸	0.743 ± 0.014	0.642 ± 0.016	0.762 ± 0.021
CE-Net ³⁹	0.796 ± 0.018	0.670 ± 0.014	0.785 ± 0.008
CPFNet ²³	0.804 ± 0.011	0.694 ± 0.009	0.800 ± 0.011
FPNN ²⁴	0.805 ± 0.017	0.672 ± 0.014	0.767 ± 0.016
Model-2	0.826 ± 0.013	0.698 ± 0.011	0.789 ± 0.016
Model-2-pos	0.528 ± 0.005	0.787 ± 0.007	0.855 ± 0.006
Proposed	0.898 ± 0.015	0.791 ± 0.007	0.859 ± 0.008

Table 3 shows the segmentation results of all models on the external test data set. The proposed model also shows the best results in all criteria. The ranking of the models corresponds to Table 3.

Table 3. Comparison of segmentation results on external ST test data set (mean ± standard deviation). The best results among all models are shown in bold.

Model	DSC	JSI	ACC
U-Net ²⁹	0.825 ± 0.011	0.747 ± 0.013	0.870 ± 0.018
UNet++ ³⁸	0.834 ± 0.005	0.750 ± 0.007	0.868 ± 0.007
CE-Net ³⁹	0.834 ± 0.016	0.774 ± 0.017	0.897 ± 0.011
CPFNet ²³	0.850 ± 0.008	0.791 ± 0.007	0.899 ± 0.008
FPNN ²⁴	0.846 ± 0.007	0.777 ± 0.007	0.884 ± 0.005
Model-2	0.831 ± 0.012	0.780 ± 0.013	0.905 ± 0.008
Model-2-pos	0.888 ± 0.002	0.827 ± 0.003	0.905 ± 0.003
Proposed	0.890 ± 0.002	0.830 ± 0.004	0.906 ± 0.005

5.1. QUALITY EVALUATION

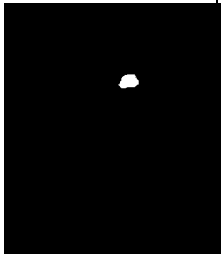

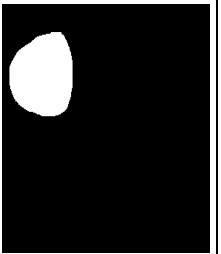

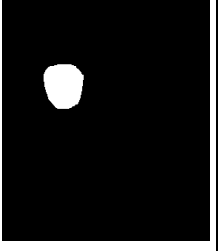
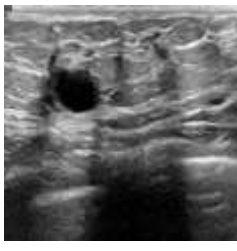
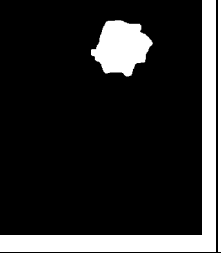

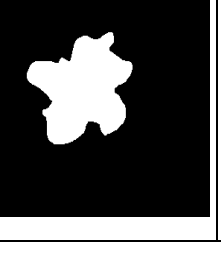

In Table 4, images from the database have been evaluated. Also, in order to quantitatively evaluate the proposed method, the output of the proposed method is placed on these images along with the Dice similarity criterion. The results of Table 5-4 show that the proposed method has the highest similarity rate of 90% and the lowest similarity rate is 89%. The results of Table 4 show that the proposed method has achieved acceptable results. The quality of this method can be discussed from two perspectives. First, the algorithm of self-encrypting networks is one of the most powerful regionalization methods and has had a great impact in improving the regionalization of breast cancer nodules. Second, the use of pre-processing methods has been able to reduce the system error to a great extent.

6. CONCLUSION

In this research, the proposed method in breast cancer detection of ultrasound images, based on the combination of deep neural network based on self-encrypting networks, was simulated on the target database, and the results of comparing the evaluation criteria of Dice similarity criterion and accuracy criterion and accuracy was obtained in various tables

and graphs, the obtained results show the superiority of the proposed method.

Table 4. Comparison of the Dice criterion in the proposed method

Dice	Proposed method output	Original image
%87		
%91		
%93		
%89		
%95		

REFERENCES

- [1] Y. Saberi, M. Ramezanpour, and R. Khorsand, "An efficient data hiding method using the intra prediction modes in HEVC," *Multimedia Tools and Applications*, vol. 79, pp. 33279-33302, 2020..
- [2] Masud, M., et al., "Pre-trained convolutional neural networks for breast chest cancer detection using ultrasound breast images." *ACM Transactions on Internet Technology (TOIT)*, 2021. 21(4): p. 1-17.
- [3] Abbasi, A., et al., "A meta-analysis of factors related to fertility attitudes, desires, and childbearing intentions in Iranian studies." *Interdisciplinary Studies in Humanities*, 2022. 14(4): p. 63-92.
- [4] Liu, M., et al., "Breast chest Histopathological Image Classification Method Based on Autoencoder and Siamese Framework." *Information*, 2022. 13(3): p. 107.
- [5] Harouni, M., M. Karimi, and S. Rafieipour, "Precise segmentation techniques in various medical images." *Artificial Intelligence and Internet of Things: Applications in Smart Healthcare*, 2021. 117.
- [6] Karimi, M., et al., "Automatic lung infection segmentation of covid-19 in CT scan images," in *Intelligent Computing Applications for COVID-19*. 2021, CRC Press. p. 235-253.
- [7] Karimi, E., A. Ebrahimi, and M.R. Tavakoli, "How optimal PMU placement can mitigate cascading outages blackouts?" *International Transactions on Electrical Energy Systems*, 2019. 29(6): p. e12015.
- [8] Karimi, M., et al., "Improving monitoring and controlling parameters for alzheimer's patients based on iomt, in Prognostic models in healthcare:" *Ai and statistical approaches*. 2022, Springer. p. 213-237.
- [9] Mahmudi, F., M. Soleimani, and M. Naderi, "Some Properties of the Maximal Graph of a Commutative Ring." *Southeast Asian Bulletin of Mathematics*, 2019. 43(4).
- [10] Arevalo, J., et al. "Convolutional neural networks for mammography mass lesion classification." in 2015 37th Annual international conference of the IEEE engineering in medicine and biology society (EMBC). 2015. IEEE.
- [11] Yap, M.H., et al., "Automated breast chest ultrasound lesions detection using convolutional neural networks." *IEEE journal of biomedical and health informatics*, 2017. 22(4): p. 1218-1226.
- [12] Karimi, M., M. Harouni, and S. Rafieipour, "Automated medical image analysis in digital mammography," in *Artificial intelligence and internet of things*. 2021, CRC Press. p. 85-116.
- [13] Harouni, M., et al., "Health monitoring methods in heart diseases based on data mining approach: A directional review," in *Prognostic models in healthcare: Ai and statistical approaches*. 2022, Springer. p. 115-159.
- [14] Moshayedi, A.J., et al., "E-Nose design and structures from statistical analysis to application in robotic: a compressive review." *EAI Endorsed Transactions on AI and Robotics*, 2023. 2(1): p. e1-e1.
- [15] Emadi, M., Z. Jafarian Dehkordi, and M. Iranpour Mobarakeh, "Improving the Accuracy of Brain Tumor Identification in Magnetic Resonance using Super-pixel and Fast Primal Dual Algorithm." *International Journal of Engineering*, 2023. 36(3): p. 505-512.
- [16] Doi, K., "Computer-aided diagnosis in medical imaging: historical review, current status and future potential. Computerized medical imaging and graphics," 2007. 31(4-5): p. 198-211.
- [17] Soleimani, M., F. Mahmudi, and M. Naderi, "Some results on the maximal graph of commutative rings. Advanced Studies:" *Euro-Tbilisi Mathematical Journal*, 2023. 16(sup1): p. 21-26.
- [18] Soleimani, M., M.H. Naderi, and A.R. Ashrafi, "TENSOR PRODUCT OF THE POWER GRAPHS OF SOME FINITE RINGS." *Facta Universitatis, Series: Mathematics and Informatics*, 2019: p. 101-122.
- [19] Brem, R.F., et al., "Evaluation of breast chest cancer with a computer aided detection system by mammographic appearance and histopathology." *Cancer: Interdisciplinary International Journal of the American Cancer Society*, 2005. 104(5): p. 931-935.
- [20] Mridha, M.F., et al., "A comprehensive survey on deep-learning-based breast chest cancer diagnosis. *Cancers*" 2021. 13(23): p. 6116.
- [21] Murthy, N.S. and C. Bethala, "Review paper on research direction towards cancer prediction and prognosis using machine learning and deep learning models." *Journal of Ambient Intelligence and Humanized Computing*, 2021: p. 1-19.
- [22] Aggarwal, R., et al., "Diagnostic accuracy of deep learning in medical imaging: A systematic review and meta-analysis." *NPJ digital medicine*, 2021. 4(1): p. 1-23.
- [23] Xie, J., et al., Deep learning based analysis of histopathological images of breast chest cancer. *Frontiers in genetics*, 2019. 10: p. 80.
- [24] Lehman, C.D., et al., "Mammographic breast chest density assessment using deep learning: clinical implementation." *Radiology*, 2019. 290(1): p. 52-58.
- [25] Le, H., et al., "Utilizing automated breast chest cancer detection to identify spatial distributions of tumor-infiltrating lymphocytes in invasive breast chest cancer." *The American journal of pathology*, 2020. 190(7): p. 1491-1504.
- [26] Navabifar, F. and M. Emadi, "A Fusion Approach Based on HOG and Adaboost Algorithm for Face Detection under Low-Resolution Images." *INTERNATIONAL ARAB JOURNAL OF INFORMATION TECHNOLOGY*, 2022. 19(5): p. 728-735.
- [27] Rehman, A., et al., "Microscopic retinal blood vessels detection and segmentation using support vector machine and K nearest

- neighbors. *Microscopy research and technique*, "2022. **85**(5): p. 1899-1914.
- [28] Cruz-Roa, A., et al., "Accurate and reproducible invasive breast chest cancer detection in whole-slide images: A Deep Learning approach for quantifying tumor extent. *Scientific reports*," 2017. **7**(1): p. 1-14.
- [29] Zhang, Q., et al., "Deep learning based classification of breast chest tumors with shear-wave elastography. *Ultrasonics*," 2016. **72**: p. 150-157.
- [30] Liu, K., et al., "Breast chest cancer classification based on fully-connected layer first convolutional neural networks." *IEEE Access*, 2018. **6**: p. 23722-23732.
- [31] Xiao, Y., et al. "Breast chest cancer diagnosis using an unsupervised feature extraction algorithm based on deep learning." in 2018 37th Chinese Control Conference (CCC). 2018. IEEE.
- [32] Xu, Y., et al., "Medical breast chest ultrasound image segmentation by machine learning. *Ultrasonics*," 2019. **91**: p. 1-9.
- [33] Minarno, A.E., et al. "CNN based autoencoder application in breast chest cancer image retrieval." in 2021 International Seminar on Intelligent Technology and Its Applications (ISITIA). 2021. IEEE.
- [34] AlEisa, H.N., et al., "Breast chest Cancer Classification Using FCN and Beta Wavelet Autoencoder." *Computational Intelligence and Neuroscience*, 2022. **2022**.
- [35] Ragab, M., et al., "Ensemble deep-learning-enabled clinical decision support system for breast chest cancer diagnosis and classification on ultrasound breast images." *Biology*, 2022. **11**(3): p. 439.
- [36] Jabeen, K., et al., "Breast chest cancer classification from ultrasound breast images using probability-based optimal deep learning feature fusion." *Sensors*, 2022. **22**(3): p. 807.
- [37] Kadam, V.J., S.M. Jadhav, and K. Vijayakumar, "Breast chest cancer diagnosis using feature ensemble learning based on stacked sparse autoencoders and softmax regression." *Journal of medical systems*, 2019. **43**(8): p.1-11.
- [38] Papież, B.W., et al. "Liver motion estimation via locally adaptive over-segmentation regularization." in *Medical Image Computing and Computer-Assisted Intervention–MICCAI 2015: 18th International Conference, Munich, Germany, October 5-9, 2015, Proceedings, Part III 18*. 2015. Springer.
- [39] Zhou, Z., et al. "Unet++: A nested u-net architecture for medical image segmentation. in *Deep Learning in Medical Image Analysis and Multimodal Learning for Clinical Decision Support*," 4th International Workshop, DLMIA 2018, and 8th International Workshop, ML-CDS 2018, Held in Conjunction with MICCAI 2018, Granada, Spain, September 20, 2018, Proceedings 4. 2018. Springer.
- [40] Duan, J., et al., "Automatic 3D bi-ventricular segmentation of cardiac images by a shape-refined multi-task deep learning approach." *IEEE transactions on medical imaging*, 2019. **38**(9): p. 2151-2164.
- [41] Feng, S., et al., CPFNet: "Context pyramid fusion network for medical image segmentation. *IEEE transactions on medical imaging*," 2020. **39**(10): p. 3008-3018.
- [42] A. Abbasi, R. Sadeghi, A. Maleki, and G. Balakhani, "A meta-analysis of factors related to fertility attitudes, desires, and childbearing intentions in Iranian studies," *Interdisciplinary Studies in Humanities*, vol. 14, no. 4, pp. 63-92, 2022.
- [43] N. Najafabadi, and M. Ramezanzpour, "Mass center direction-based decision method for intraprediction in HEVC standard." *Journal of Real-Time Image Processing*, vol. 17, no. 5, pp. 1153-1168, 2020.
- [44] B. Heidari, and M. Ramezanzpour, "Reduction of intra-coding time for HEVC based on temporary direction map." *Journal of Real-Time Image Processing*, vol. 17, pp. 567-579, 2020.
- [45] A. Rehman, M. Harouni, F. Zogh, T. Saba, M. Karimi, and G. Jeon, "Detection of Lung Tumors in CT Scan Images using Convolutional Neural Networks." *IEEE/ACM Transactions on Computational Biology and Bioinformatics*, 2023.
- [46] M. Karimi, M. Harouni, E. I. Jazi, A. Nasr, and N. Azizi, "Improving monitoring and controlling parameters for alzheimer's patients based on iomt," *Prognostic models in healthcare: Ai and statistical approaches*, pp. 213-237: Springer, 2022.
- [47] F. Mahmudi, M. Soleimani, and M. Naderi, "Some Properties of the Maximal Graph of a Commutative Ring," *Southeast Asian Bulletin of Mathematics*, vol. 43, no. 4, 2019.
- [48] M. Karimi, M. Harouni, and S. Rafieipour, "Automated medical image analysis in digital mammography." *Artificial intelligence and internet of things*, pp. 85-116: CRC Press, 2021.
- [49] M. Harouni, M. Karimi, A. Nasr, H. Mahmoudi, and Z. Arab Najafabadi, "Health monitoring methods in heart diseases based on data mining approach: A directional review." *Prognostic models in healthcare: Ai and statistical approaches*, pp. 115-159: Springer, 2022.
- [50] A. J. Moshayedi, A. S. Khan, Y. Shuxin, G. Kuan, H. Jiadong, M. Soleimani, and A. Razi, "E-Nose design and structures from statistical analysis to application in robotic: a compressive review." *EAI Endorsed Transactions on AI and Robotics*, vol. 2, no. 1, pp. e1-e1, 2023.
- [51] M. Emadi, Z. Jafarian Dehkordi, and M. Iranpour Mobarakeh, "Improving the Accuracy of Brain Tumor Identification in Magnetic Resonance using Super-pixel and Fast Primal Dual Algorithm." *International Journal of Engineering*, vol. 36, no. 3, pp. 505-512, 2023.
- [52] M. Emadi, M. Karimi, and F. Davoudi, "A Review on Examination Methods of Types of Working

- Memory and Cerebral Cortex in EEG Signals."** Majlesi Journal of Telecommunication Devices, vol. 12, no. 3, 2023.
- [53] E. Karimi and A. Ebrahimi, "**Probabilistic transmission expansion planning considering risk of cascading transmission line failures.**" International Transactions on Electrical Energy Systems, vol. 25, no. 10, pp. 2547-2561, 2015.
- [54] E. Karimi and A. Ebrahimi, "**Considering risk of cascading line outages in transmission expansion planning by benefit/cost analysis.**" International Journal of Electrical Power & Energy Systems, vol. 78, pp. 480-488, 2016.